JES Focus Issue on Progress in Molten Salts and Ionic Liquids

Influence of Electrode Gas Flow Rate and Solid Oxide Ratio in Electrolyte on the Seebeck Coefficient of Molten Carbonate Thermocell

S. Kandhasamy,[a,*] L. Calandrino,[b] O. S. Burheim,[c,] A. Solheim,[d] S. Kjelstrup,[e] and G. M. Haarberg[a,**,z]**

[a]*Department of Materials Science and Engineering, Norwegian University of Science and Technology (NTNU), Trondheim, Norway*
[b]*Department of Mechanical and Industrial Engineering, University of Brescia, Brescia, Italy*
[c]*Department of Electrical Engineering and Renewable Energy, NTNU, Trondheim, Norway*
[d]*SINTEF Materials and Chemistry, SINTEF, Trondheim, Norway*
[e]*Department of Chemistry, NTNU, Trondheim, Norway*

Thermocells represent a promising way to utilize heat as a power source. The aim of this work is to develop a thermocell with identical gas electrodes using molten carbonate-based electrolytes. The cell can generate power from waste heat, and can also utilize the CO_2 rich off-gas available in metal producing industries. The flow rate of the gas supply to the electrodes needs to be optimized. Its effect on the Seebeck coefficient was not studied systematically before. The addition of solid oxide to the molten carbonate melt alters also the system's Seebeck coefficient. We report measurements where we vary the content of solid oxide in the liquid eutectic electrolyte mixture as well as the electrode gas flow rate. The Seebeck coefficient is reported for various ratios of eutectic $(Li,Na)_2CO_3$ molten carbonate and dispersed solid oxide MgO, and for varying gas ($CO_2|O_2$) flow rates to the electrode interfaces.
 [DOI: 10.1149/2.0391708jes]

Manuscript submitted February 15, 2017; revised manuscript received June 1, 2017. Published June 14, 2017. This was Paper 3465 presented at the Honolulu, Hawaii, Meeting of the Society, October 2–7, 2016. *This paper is part of the JES Focus Issue on Progress in Molten Salts and Ionic Liquids.*

Thermoelectric systems converting heat into electricity are well known since their discovery of the Seebeck effect in 1821.[1] The thermoelectric power was first demonstrated for aqueous thermogalvanic cells, Quickenden et al. summarized many similar systems in a review.[2] However, because of their low figure of merit, due to the high thermal conductivity of water and their low operating temperature, they were not further investigated. Industrial metal production is associated with production of large amounts of thermal energy and high CO_2 emissions. Large amounts of heat are wasted by dissipation in the surroundings. Thermoelectric converters based on semiconductor materials may be used to generate electricity from such waste heat and Seebeck coefficients of 0.8 mV/K are typical.[3] However, the materials used in these devices are often scarce and expensive. The use of an ion-conducting electrolyte and gas electrodes offers possibilities of achieving high Seebeck coefficients.[4–6] Electrolytes such as ionic liquids and molten salts offer possibilities of higher stable operating temperatures and larger Seebeck coefficients than semiconductor thermoelectric materials.[7,8] Experimental studies of electrochemical cells with inexpensive components such as molten carbonate electrolyte and $CO_2|O_2$ gas electrodes have been reported earlier. Seebeck coefficients in the range of −1.25 mV/K at average cell temperature of 750°C were obtained.[9,10]

A thermocell is an electrochemical system with identical electrodes placed at different temperatures in an electrolyte solution. In multicomponent mixtures, thermal diffusion is set up due to the temperature gradient between the electrodes. Ion transport between the electrodes due to the thermal driving force leads to a potential difference.[2] At steady state condition, a Soret equilibrium is achieved after a certain time. Seebeck coefficients are determined by measuring the initial as well as the steady state potential when a negligible current is passing through the cell.

A thermocell was demonstrated with different cell components, as metal/gas electrodes with liquid/solid electrolytes.[11] A small Seebeck coefficient was observed with metal electrodes M, in the thermocell M(T) | MX | M(T+ΔT), here MX is the electrolyte with ions M^+ and X^-. Here T is the left hand side temperature and ΔT is the temperature difference between the electrodes. Dendrite growth, corrosion, and polarization may affect the thermoelectric conversion under operation. Gaseous electrodes X, like in the thermocell X(T) | MX | X(T+ΔT) are free from the above-mentioned deficiencies. Furthermore, the use of gas electrodes, include larger reaction entropies. Such electrodes may therefore deliver a higher electric potential than a thermocell with metal electrodes.[12,13] The Seebeck coefficient of thermocells depends on the change in entropy of the half-cell reaction. The gas at the hot electrode, ionize and the cation is transported through the electrolyte to the cold electrode where the reverse reaction happens. The entropy change of the half-cell reaction is large, mainly because gas molecules disappear or appear. Important aspects for selection of electrolyte are the boiling point, a low vapor pressure, high electrical conductivity, low thermal conductivity and fast kinetics of the gas electrode. In favorable cases, the electrolyte mixture contains a reaction product of the electrode gas. This means chlorine from chloride melts, oxygen from an oxide containing electrolyte and carbon dioxide from molten carbonate mixtures.[14,15]

In this study, a gas mixture of $CO_2|O_2$ is used in the electrode gas to obtain a reversible electrode reaction. The reaction introduces the carbonate ion in a molten carbonate electrolyte mixture with solid-state MgO dispersed. The use of solid MgO in a molten carbonate was first reported by Jacobsen et al.[5] Addition of a certain quantity of Al_2O_3 in molten AgI was reported to increase the ionic conductivity and the thermoelectric power.[16] The presence of a solid phase oxide matrix may reduce the heat flux between the electrodes. The so-called "figure of merit" is related to the thermoelectric power generation efficiency. It increases with an increasing Seebeck coefficient, a decreasing thermal conductivity and a decreasing electrical resistivity.[2] The use of non-critical and non-poisonous materials and the prospective of a high thermoelectric efficiency, as well as the availability of CO_2 gas, may be advantageous for the thermocell compared to semiconductor thermoelectric devices. The change in the Seebeck coefficient for similar thermocells with different carbonate melt compositions, electrode gas mixture, current collector, solid-state oxide and various average cell

*Electrochemical Society Student Member.
**Electrochemical Society Member.
[z]E-mail: geir.martin.haarberg@ntnu.no

Table I. Electrode gas flow rate and MgO to carbonate ratio used in the experiments.

Cell Label		CO_2 / O_2 Flow rate		Weight %		Volume %	
		Scale Reading (NML/M)	Scale Conversion (ml/min)	MgO	Eutectic Mixture $Li_2CO_3 + Na_2CO_3$	MgO	Eutectic Mixture $Li_2CO_3 + Na_2CO_3$
Electrode Gas Flow Rate	A	40	14.7	55	45	44.3	55.7
	B	50	16.1				
	C	60	18.6				
	D	70	21.0				
	E	80	23.4				
Differential Ratio of MgO in Electrolyte	D	70	21.0	55	45	44.3	55.7
	F			65	35	54.7	45.3
	G			75	25	66.1	33.9
	H			85	15	78.7	21.3

temperature has been reported before.[5,9,10] The content of the solid MgO phase and the flow velocity of electrode gas may influence the thermoelectric potential. This was not reported before, and was systematically investigated in this work.

Theoretical Considerations

The electrochemical cell with gas electrodes, reversible to the carbonate ion, held at different temperatures can be represented as:

$$\mathrm{Au}\,(T^{s,a})\,|\mathrm{CO_2}\,(g)\,,\,\mathrm{O_2}\,(g)|\,(\mathrm{Li,\,Na})_2\mathrm{CO_3}\,(l)\,,$$

$$\mathrm{MgO}\,(s)\,|\mathrm{CO_2}\,(g)\,,\,\mathrm{O_2}\,(g)|\,\mathrm{Au}\,(T^{s,c})$$

The electrochemical reaction at the left-hand side electrode is:

$$2\,\mathrm{CO_3^{2-}}\ (l) \rightarrow 2\,\mathrm{CO_2}\ (g) + \mathrm{O_2}\ (g) + 4e^- \qquad [1]$$

The reverse reaction takes place at the right-hand side. The Seebeck coefficient for the cell with uniform (homogeneous electrolyte) melt composition (short time) is:

$$\alpha_S = \left(\frac{\Delta\varphi}{(T^{s,c} - T^{s,a})}\right)_{j=0,\ t=0}$$

$$= -\frac{1}{F}\left[\frac{1}{2}\,S_{CO_2} + \frac{1}{4}\,S_{O_2} + S_e^* - \frac{1}{2}\,S^*_{CO_3^{2-}} + \left(\frac{t_2}{x_2} - \frac{t_1}{x_1}\right)\frac{q^*}{T}\right] \qquad [2]$$

where S_j is the entropy of component j at average temperature of the electrodes T and pressure p_j. The terms S_e^* and $S^*_{CO_3^{2-}}$ are the transported entropy of the electron and carbonate ion, respectively. The entropies and the transported entropies are generally functions of temperature. The gas entropies are expected to be larger than the transported entropies. These terms have then a negative contribution to the Seebeck coefficient. Then t_1, t_2 are the transference coefficient and x_1, x_2 are the mole fractions of Li_2CO_3 and M_2CO_3. The ratio $\frac{q^*}{T}$ may be interpreted in terms of enthalpy changes across the layer, but it is difficult to interpret the sign of this last term. If the term is positive, the Seebeck coefficient at initial times is more negative than at infinite time, when the last term disappears. A detailed theoretical derivation of the equation based on non-equilibrium thermodynamics is explained in our previous work.[9,10]

Experimental

Lithium carbonate (Li_2CO_3), sodium carbonate (Na_2CO_3) and magnesium oxide (MgO) were purchased from Sigma-Aldrich with purity > 99%. The MgO powder has the average particle size of ~2.8 μm, measured in a laser scattering particle size distribution analyzer. Pre-made electrode gas mixtures containing 34% oxygen mixed with carbon dioxide were obtained from AGA, Norway. Gold sheet and wire for the electrodes and wires of platinum, platinum with 10% rhodium for thermocouple fabrication were obtained from K.A. Rasmussen, Norway. Alumina tubes (5 mm outer diameter and 550 mm length) with one center bore of diameter 2.3 mm and four other bores with 0.75 mm diameter and a tubular crucible (inner diameter of 38 mm with 200 mm length) were obtained from MTC Haldenwanger, Germany. The flow rate of electrode gas supplied through the ceramic tubes was controlled by a pair of Brooks Instrument Sho-Rate meters with ±5% accuracy, both the scale reading and appropriate flow conditions for the gas used are shown in Table I. The temperature of the electrodes and the cell potential were recorded every 10 seconds by using Agilent, 34972A data acquisition unit.

The thermocell was placed inside a standard laboratory vertical tubular furnace as shown in Figure 1. The cell consisted of an Al_2O_3 tubular crucible, with two electrodes immersed in a molten carbonate electrolyte mixture. In each alumina tube, the gold wire was inserted into the center bore (diameter 2.3 mm) of a 5-bore Al_2O_3 tube and the gold sheet (5 × 5 mm) was spot-welded to the wire. The thermocouple (Pt-Pt10%Rh) was inserted into two of the other holes (diameter 0.75 mm) and the junction was positioned as near as possible to the gold sheet. $CO_2|O_2$ gas was supplied through the bores of the ceramic tube. The electrolytes mixture was prepared by mixing the molten carbonates and MgO by hand in a mortar. The mixture was dried for

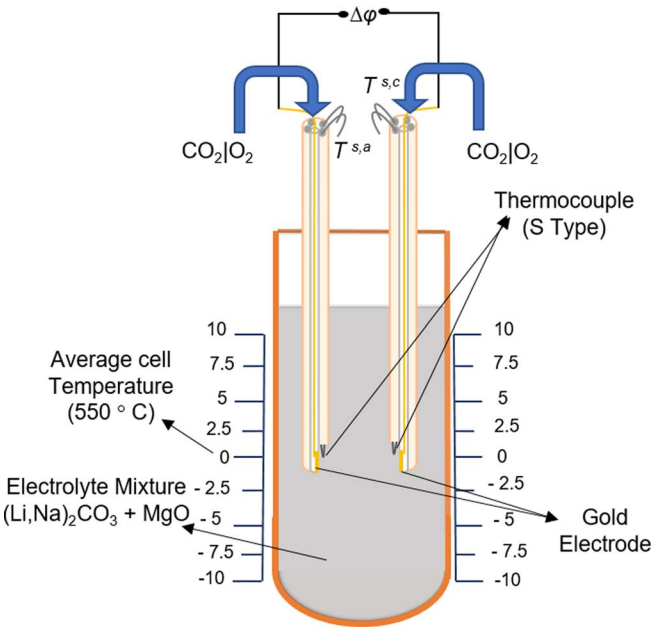

Figure 1. Cross sectional view of the thermocell with reference scale for positioning the electrode to create the required temperature gradient. (Electrode positions for ΔT of 20°C was $T^{s,a}$ and $T^{s,c}$ at 10 and −10 position respectively, vice versa for ΔT of −20°C).

Table II. Seebeck coefficient of the cells with varying electrode gas flow rate and average temperature 550°C.

Cell Label	CO_2 / O_2 Flow rate (ml/min)	Volume % MgO	Volume % Eutectic Mixture Li_2CO_3+Na_2CO_3	Seebeck Coefficient (mV/ K) Slope	Seebeck Coefficient (mV/ K) Standard Error
A	14.7	44.3	55.7	−1.1	0.03
B	16.1			−1.2	0.02
C	18.6			−1.6	0.03
D	21.0			−1.7	0.05
E	23.4			−1.0	0.03

more than 48 hours at 200°C. Then the electrolyte was melted under a nitrogen atmosphere at 550°C in the vertical tube furnace at least for 48 hours to ensure stable conditions. The ratio of Li_2CO_3 and Na_2CO_3 eutectic mixture and the dispersed solid MgO in the electrolyte mixture, as well as the $CO_2|O_2$ gas flow rate at the electrode/electrolyte interface, are listed in Table I for the different cells.

A temperature difference (ΔT) was established between the electrodes by positioning them at different heights in the crucible. The average cell temperature was kept at 550°C and the temperature difference was always smaller than 20°C. The cell potential was measured as a function of the temperature difference, after an equilibration period of 15–20 min followed by a measurement with a new temperature difference. Recordings were made over some 50 minutes time at a certain temperature difference to make sure that the measured potential was stable. This is then taken as an initial time measurement. The cell measurements were performed using the same procedure as in our previous reports.[9,10] At infinite time (meaning days) the last term in the Equation 2 disappears.

The measurement conditions and the cases investigated are listed in Table I. The table shows that we varied the MgO (s) content in the melt and the gas flow rate, keeping the electrolyte carbonate melt composition equal to the eutectic.

The phase analysis of the electrolyte mixture was carried out before and after thermocell measurements, using Bruker-D8 ADVANCE X-ray diffraction (XRD) with CuKα radiation (λ = 1.5406 Å). The elemental composition was also determined on the same samples by Energy Dispersive Spectroscopy (EDS) using an Oxford instrument Aztec EDS system attached to a Hitachi S-3400N Scanning Electron Microscopy (SEM). The front beryllium window in the detector absorbs low-energy X-rays. Thus, EDS cannot detect the presence of elements with atomic number less than 5 which includes Li, while all other possible elements in the electrolyte mixture were detected. The particle size distribution of the solid-state MgO powder was measured in Horiba LA-960 laser scattering particle size distribution analyzer, by dispersing the MgO powder in ethanol using ultra sonic bath.

Results and Discussion

The results are presented in Tables II and III and Figures 2–6. The tables summarize results from the figures, for the case studies A-G listed in Table I. We consider first the structure information on the system to have a background for discussion of the experimental results for the Seebeck coefficient variations.

Homogeneity of the electrolyte mixture.—The X-ray diffraction results of the electrolyte samples of Cells D and G, collected from various regions in the cell after the experiments are shown in Figures 2a and 2b. The indistinguishable XRD patterns for the samples from the different regions (top, middle, bottom) confirm that the whole electrolyte mixture is homogeneous. A significant reduction in peak intensity of the molten carbonate can, however, be seen when we compare results from before (Figure 2c) and after (Figure 2a) the thermocell experiment. This can be understood as a poorer crystallinity of the carbonate mixture, attained during re-solidification in the presence of solid oxide. The absence of additional peaks before (Figure 2c) and after (Figure 2a) the thermocell measurements, suggests also that impurities are absent. That is, they have not been added in the melting or cooling process. From this absence, we can also conclude that electrolyte decomposition or carbonate reactions with MgO do not happen to any significant degree.[17]

The results from the EDS analysis on the used electrolyte are shown in Figure 2d. They present more accurate information about elemental distribution than the XRD analysis. The EDS results in Figure 2d are average values from the analysis, over at least two different locations of each sample. Observations after the experiment in cell G indicate a ∼3–5 wt% higher concentration of MgO at the bottom of the cells. This cell has a MgO content of 66.1%, see Table II. But at the concentration used in most cells, 44.3% MgO (Cell D), the concentration is uniform. The extra solid phase at the bottom of cell G indicates that the dispersion has reached a solubility limit. Homogeneity seems to be maintained throughout the measurement with moderate content of MgO(s), <66.1% with gas flow rates below 21 ml/min.

These data altogether support the idea that there are no side reactions or concentration gradients in the electrolyte during the experiments listed in Table II, and that Equation 2 applies. Further support for Equation 2 is obtained from the estimated time to reach Soret equilibrium. Recent simulations provide a diffusion coefficient of Li^+ in Li_2CO_3 at 550°C equal to $D = 1.4\ 10^{-9}$ m^2/s.[18] The distance between the electrodes $h = 3.8$ cm. The system characteristic relaxation time is therefore $\theta = h^2/(\pi^2 D) = 29$ hrs, cf. Kang et al.[9] The stationary state value is reached after a time several times this value, i.e. several days. The steady state was obtained in our experiments within an order of magnitude 50 minutes, which then can be seen as an initial time measurement, compatible with the finding of uniform concentrations (see above).

Reversibility of the electrodes.—We have further found by inspecting the raw data, like the ones pictured in Figure 3a and processes in Figure 3b, that the thermoelectric potential measurement could be reversed by reversing the temperature difference, and that there was no bias potential between the gold electrodes at moderate flows of gas to the electrode. Gold was chosen to avoid interference of oxide layers, which are common on Pt. The straight line in Figure 3b allows us to conclude that the potential measurement is sound (reversible, well defined); and that the standard deviation between 3 and 6% in Tables II and III in the line reflects the accuracy of the experiment.

The Seebeck coefficient and the electrode gas flow rate.—The thermoelectric potentials, recorded for cells A-E at an average operating temperature of 550°C, are presented in Table II. All the potentials were plotted against the respective temperature difference, as in Figure 3b, and the Seebeck coefficient was calculated from the slope of the linear fit. The Seebeck coefficient at a slow flow rate of electrode gas (16.1 ml/min) was similar to a previously reported value, ∼−1.2 mV/K, cf. Table II.[9,10]

Table III. Seebeck coefficient of the cells with different ratio MgO in electrolyte and average temperature 550°C.

Cell Label	CO_2 / O_2 Flow rate (ml/min)	Volume % MgO	Volume % Eutectic Mixture Li_2CO_3+Na_2CO_3	Seebeck Coefficient (mV/K) Slope	Seebeck Coefficient (mV/K) Standard Error
D	21.0	44.3	55.7	−1.7	0.05
F		54.7	45.3	−1.7	0.04
G		66.1	33.9	−1.7	0.06

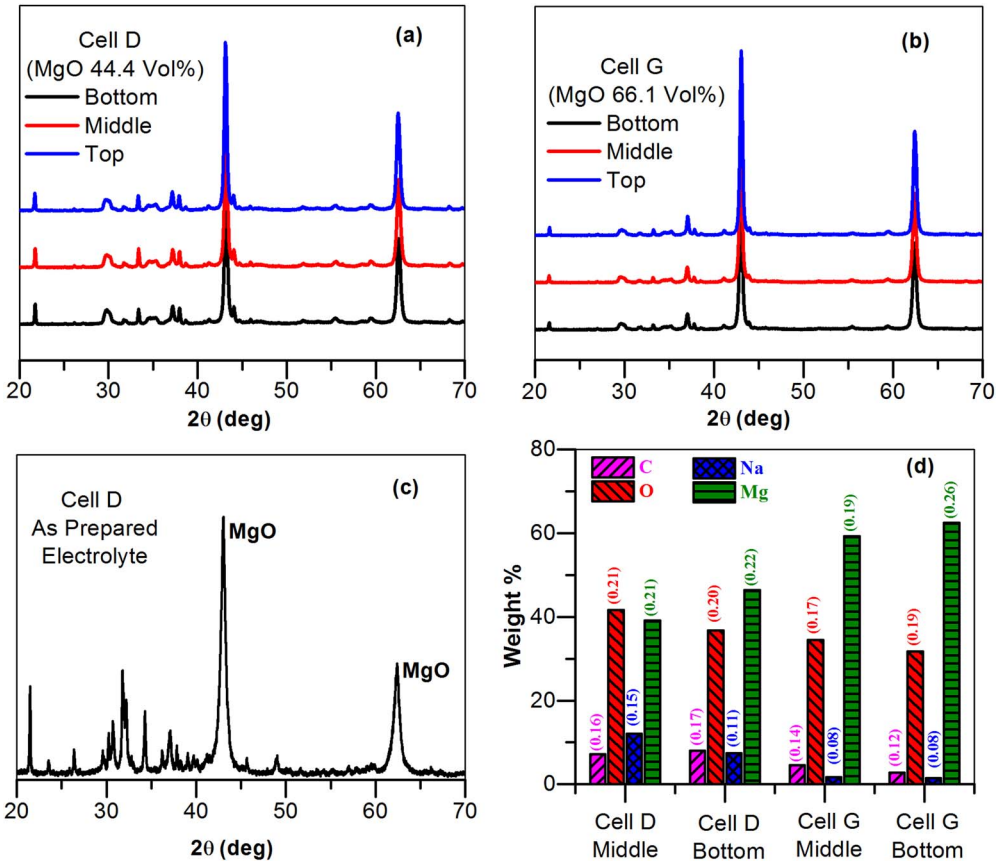

Figure 2. X-ray diffraction patterns for the electrolyte mixer after (a,b) and before (c) thermocell measurement. (d) EDS elemental analysis of the electrolyte after thermocell measurement (respective wt% sigma error value was mentioned in the bracket).

When we exclude the results for cell E in Table II, reasons will be discussed later, the Seebeck coefficient of Table II and Figure 3 varied systematically from cell A (−1.1 mV/K) to cell D (−1.7 mV/K) with an increasing gas flow rate. Each result was stable for more than an hour, see Figure 4. Figure 5 shows an experiment with constant temperature difference, held over 3 hours. Some fluctuations in the temperature were observed. We attribute them to changes in bubble coverage at times when the gas flow rate was changed. A huge change in initial potential was, however, observed by increasing the gas flow stepwise from 0 to 70 ml/min. This is the origin of the varying Seebeck coefficient in Table II.

This systematic dependence of the potential on the gas flow rate is, however, difficult to understand, since we found no significant bias potential (see discussion above). Normally an increased flow gives a better stirring and elimination of concentration polarization or thermal polarization (Soret effects). However, in this situation, there is no concentration polarization to reduce. There is a zero-bias potential at zero temperature difference. The well-behaved thermoelectric potential measurements (Figure 3) indicate that the electrode gas seems to have achieved the temperature of the gold electrodes. Any lack of electric contact and ill-defined electrode reactions, cannot explain these results which seem to be reversible. Similar cells, with halide

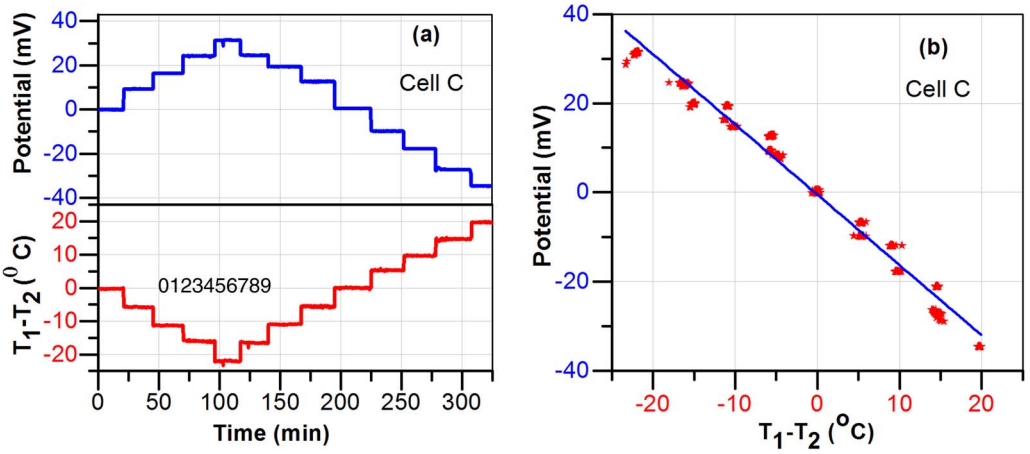

Figure 3. (a) The measured potential and temperature difference and, (b) Seebeck coefficient plot for cell C with electrode gas flow rate of 18.6 ml/min.

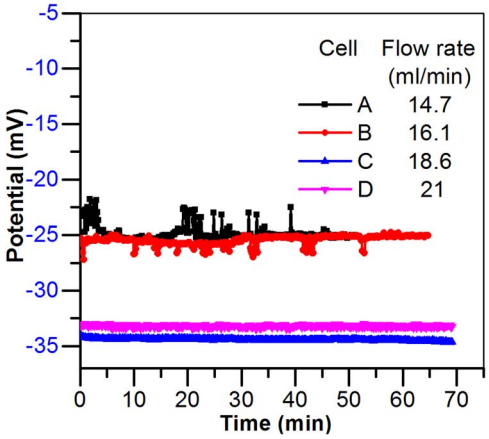

Figure 4. Measured potential versus time for electrode temperature difference of 20°C with varying electrode gas flow rate (Cell A-D).

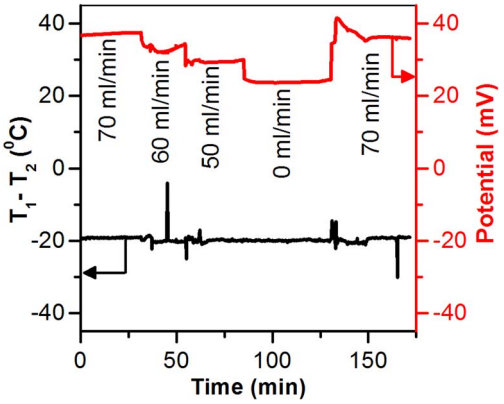

Figure 5. Potential measured with a thermocell, at constant electrode position with change in gas flow rates.

electrolyte and halogen electrodes, have shown similar behavior. Metz et al.,[19] suggested that the Seebeck coefficient varied with gas flow rate because of lack of contact area at the electrode interface and depolarization effects. This may be so in the case of cell E which breaks down (see below), but not in cells A-D. At this moment, we have therefore no scientifically justified explanation for the effect.

The three-phase contact area at the electrode-gas-electrolyte interface needs to be well equilibrated and mixed to give a reliable potential reading. It is, however, difficult if not impossible, to stir the molten electrolyte with 44.3 volume % of MgO dispersed. This fact could, however, lead to flow-dependent systematic differences between the two electrodes. A tentative explanation is then that electrokinetic effects arise. Such effects may add to the electric potential, for instance, if the gas pressure differs between the two sides. Gas flow over a heated sensing plate is known to give a difference in electric potential between the ends of the plate, meaning that the gas flow velocity can be found with high precision and quick response time from a Seebeck coefficient.[20,21] More research is needed to investigate these variables.

Inhomogeneities of the electrolyte mixture and lack of reversibility of electrodes.—From Figures 2a–2c and Figure 3a, 3b we concluded above that the system responded in a predictable way, for an initial time measurement (absence of Soret effects). The results from Cell G (Figure 2d) and Table II confirmed that there is an optimal concentration of MgO(s) in the dispersion. The value should be <66.1%. It is known from the literature (Jacobsen et al.),[5] and we have also confirmed this, that the system is more stable with than without the solid oxide dispersed.[10] The value 44.3% MgO was used in the original work by Jacobsen et al.[5] The Seebeck coefficient with pure Li-carbonate was −0.88 mV/K, while with MgO(s) dispersed in the Li-carbonate it rose to −1.04 mV/K.[10] The presence of MgO has clearly an impact on the Seebeck coefficient.

In order to investigate this, further, we studied the effect of increasing the content of MgO. Table II shows results for increasing content of MgO(s), from 44.3 to 66.1% (cells D, F, G). The mixture is no longer homogeneous at the higher concentration (Figure 2d). However, the Seebeck coefficient is unchanged (−1.7 mV/K). Going beyond the value of 66.1%, to 78.7%, has a detrimental effect. The electric potential is then no longer a linear function of the temperature difference. Figure 6 shows how we move from a predictable (Figure 6a) to an unpredictable cell behavior (Figure 6b) by overloading the dispersion with MgO(s). We may speculate that an overload may obstruct the electrode reactions i.e. by preventing contact of components, leading again to ill-defined electrode reactions.

The high Seebeck coefficient (−1.7 mV/K) makes it interesting to pursue the track of adding solid state compounds. Shahi et al.[16] reported that the ionic conductivity increased with the addition of Al_2O_3 in molten AgI until 30 mole%, but decreased on further additions. An increase in thermoelectric power was also observed for Al_2O_3 dispersed in AgI, compared to pure AgI.[16] Clearly, this is a topic for further research.

Conclusions

The Seebeck coefficient of molten carbonate thermocells with suitable gas electrodes was measured at 550°C, and with MgO(s) dispersed in a Li-Na eutectic mixture of carbonates. The Seebeck co-

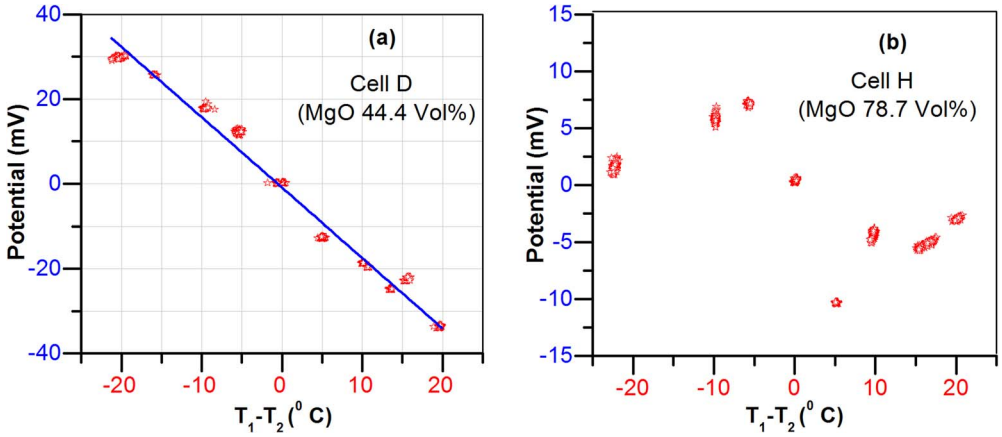

Figure 6. (a) Seebeck coefficient plot for cell D, and (b) Measured potential versus temperature difference in the cell H.

efficient of −1.7 mV/K remains unchanged for different electrolyte mixtures with 44 to 66 volume% of MgO(s) dispersed in the eutectic carbonates. An optimal gas flow rate will help maintain electrolyte homogeneity, as evidenced by XRD and EDS studies, as well as good electrolyte/electrode contacts.

Acknowledgment

The authors wish to acknowledge the Research Council of Norway and industrial partners Hydro Aluminium, Boliden, Glencore, and Permascand for financial support in the research project "Sustainable and Energy Efficient Electrochemical Production and Refining of Metals (SUPREME)".

References

1. E. Bouty, *J. Phys. Theor. Appl.*, **9**, 229 (1880).
2. T. I. Quickenden and Y. Mua, *J. Electrochem. Soc.*, **142**, 3985 (1995).
3. M. H. Elsheikh, D. A. Shnawah, M. F. M. Sabri, S. B. M. Said, M. H. Hassan, M. B. Ali Bashir, and M. Mohamad, *Renew. Sustain. Energy Rev.*, **30**, 337 (2014).
4. K. Cornwell, *J. Phys. D. Appl. Phys.*, **1**, 173 (1968).
5. T. Jacobsen and G. H. J. Broers, *J. Electrochem. Soc.*, **124**, 207 (1977).
6. B. Burrows, *J. Electrochem. Soc.*, **123**, 154 (1976).
7. Y. Ito and T. Nohira, *Electrochim. Acta*, **45**, 2611 (2000).
8. Y. V. Kuzminskii, V. A. Zasukha, and G. Y. Kuzminskaya, *J. Power Sources*, **52**, 231 (1994).
9. X. Kang, M. T. Børset, O. S. Burheim, G. M. Haarberg, Q. Xu, and S. Kjelstrup, *Electrochim. Acta*, **182**, 342 (2015).
10. M. T. Børset, X. Kang, O. S. Burheim, G. M. Haarberg, Q. Xu, and S. Kjelstrup, *Electrochim. Acta*, **182**, 699 (2015).
11. K. Cornwell, *J. Phys. D. Appl. Phys.*, **5**, 1199 (1972).
12. J. L. Weininger, *J. Electrochem. Soc.*, **111**, 769 (1964).
13. S. Senderoff and R. I. Bretz, *J. Electrochem. Soc.*, **109**, 56 (1962).
14. S. Senderoff, *U.S. Pat.*, 3,294,585 (1966).
15. H. Holtan, *J. Chem. Phys.*, **19**, 519 (1951).
16. K. Shahi and J. B. Wagner, *J. Electrochem. Soc.*, **128**, 6 (1981).
17. M. Mizuhata, Y. Harada, G. Cha, A. B. Béléké, and S. Deki, *J. Electrochem. Soc.*, **151**, E179 (2004).
18. D. Roest, *Brage.bibsys.no* (2016).
19. C. R. Metz and R. L. Seifert, *J. Electrochem. Soc.*, **117**, 49 (1970).
20. N. Kockmann, *Encyclopedia of Microfluidics and Nanofluidics*, p. 3279, Springer, New York (2015).
21. A. K. Sood and S. Ghosh, *Phys. Rev. Lett.*, **93**, 86601 (2004).